LAWRENCE
LIVERMORE
NATIONAL
LABORATORY

LLNL-CONF-425261

High-Power Electrostatic Discharges in PETN: Threshold and Scaling Experiments

W. Liou, J. F. McCarrick, R. L. Hodgin, D. F. Phillips

March 9, 2010

14th International Detonation Symposium
Coeur d'Alene, ID, United States
April 11, 2010 through April 16, 2010

Disclaimer

High-Power Electrostatic Discharges in PETN: Threshold and Scaling Experiments

William Liou*, James F. McCarrick*, Ralph L. Hodgin* and Danial F. Phillips*

*Science and Technology Principal Directorate
Lawrence Livermore National Laboratory, Livermore, CA 94551

Abstract. There is a considerable set of data establishing the safety of PETN-based detonators that are insulted by electrostatic discharge (ESD) from a human body. However, the subject of ESD safety has garnered renewed interest because of the sparse data on high-power, low-impedance discharges that result when the source is a metallic object such as a tool. Experiments on as-built components, using pin-to-cap fault circuits through PETN-based detonators, showed significant evidence of a power dependence but with a very broad energy threshold and some uncertainty in the breakdown path. We have performed a series of experiments using a well-defined arc discharge path and a well-characterized source that is capable of *independent* variation of energy and power. Studies include threshold variation with power, arc length, powder surface area, and surface vs. bulk discharge paths. We find that an energy threshold variation with power does not appear to exist in the tested range of fractions to tens of MW, and that there are many subtleties to proper energy and power bookkeeping. We also present some test results for PBX 9407.

Introduction

The study of the safety of high explosives subjected to electrostatic discharge (ESD), especially in the context of detonators, is far from a new topic. There exists a large body of test data and protocols particularly in the context of ESD resulting from contact with a human body, and the published literature has some excellent points of entry to those new to the topic.[1] However, for all of the prior work done, there are sufficient number of complications and variations that require many issues to be further investigated. Spurred by results from "as-built" ESD testing of exploding bridge wire (EBW) detonators, we focus in this work on *power dependence* of the energy threshold of low-density PETN (pentaerythritol tetranitrate), as explored with a novel fireset configuration.

Historical As-Built LLNL Tests

In the 2003-2007 time frame, a series of tests were performed at Lawrence Livermore National Laboratory (LLNL) to measure the energy threshold of exploding bridge wire (EBW) and exploding bridge foil (EBF) detonators subjected to "furniture" ESD (FESD) insults.[2] We refer to these tests as "historical" because they set the stage for the current work.[a] In a FESD insult scenario, the detonator is contacted by a charged metallic source that does not have the high source

[a] Unfortunately, to the authors' knowledge, formal publication of the historical test results has not yet occurred.

impedance of the human body,[3,4] and thus can deliver a higher fraction of the available source energy to the high explosive. In a typical scenario, a common-mode high voltage is applied to the exposed detonator cables, and electrical breakdown takes place from the bridge to the metallic detonator cap, which is assumed in a worst-case safety scenario to be electrically grounded (e.g., by sitting on a large metal work surface or by being installed in a larger operational fixture). The breakdown path can either be through the bulk of the detonator HE or along the surface that typically exists between the HE and the header structure holding the bridge. In the LLNL tests, the detonators contained low-density PETN and the observed energy thresholds, when scaled per unit length of arc, were of the same order as those observed previously by Tucker.[5] However, the thresholds appeared to vary significantly with the inductance of the source circuit, which could impact safety studies where the source inductance is not known and conservative assumptions must be made. It was assumed that the variation in circuit inductance drove a more fundamental variation in power delivered to the HE. This is discussed further in the section *Interpretation of Historical As-Built Tests* below.

Flexible Fireset

To better understand the power dependence, we have constructed a fireset with the following features: 1) independently swappable discrete source capacitors and inductors to decouple variations in energy and power; 2) a fast, low-impedance mechanical tack switch to decouple the charge voltage from the internal breakdown strength; 3) an integrated and minimally perturbing current-viewing resistor; and 4) a well-defined point-to-point arc path.

We discuss further details of the fireset design, operation, and characterization in the section *Fireset Hardware* below.

Interpretation of Historical As-Built Tests

We will repeat here enough details of the historical tests to provide motivation for the current work; however, it is not our intent to provide a complete description of those experiments. The as-built tests used hemispherical EBW and EBF detonators with identical HE pressings: an inner low-density pressing of PETN and an outer pressing of PBX 9407, which is a high-density RDX-based secondary explosive. The PETN powder properties, such as specific surface area, were not characterized. Schematics of the cross sections are shown in Figure 1.

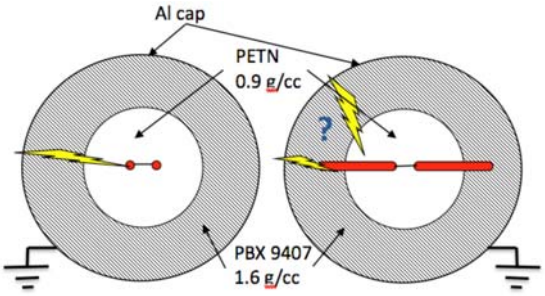

Fig 1. Schematic cross section of the bridge/header interface of the hemispherical EBW (left) and EBF (right) detonators in the historical LLNL tests.

The results of three go/no-go test series are shown in Figure 2, displayed as a function of the circuit inductance for that test series. The firesets were essentially completely rebuilt between each series, each time with a different optimization to reduce the inductance, which was characterized by fitting current waveforms measured with a current-viewing transformer (CVT). Within each series, there is considerable overlap between the goes and no-goes, but a trend of lowering threshold does appear to emerge as the circuit inductance is dropped. Since real geometries subject to FESD insults do not need space for experimentally necessary switches and standoff to protect reusable components, the possibility of real fault circuits of comparable or lower inductance to those tested (and therefore even lower energy thresholds) is raised.

Note from Figure 1 that the shortest possible breakdown path in the EBF configuration crosses only PBX 9407. The speculation was that, in the high-power regime, it might be possible to initiate a high-density explosive with relatively low total source energy. However, as discussed later in this paper, this does not appear to be the case; instead, one must conclude that the electrical breakdown in the EBF tests was not nearly as simple as “the

shortest path" since it must have crossed PETN in order to produce a violent reaction. This uncertainty in arc length further complicates interpretation of the results.

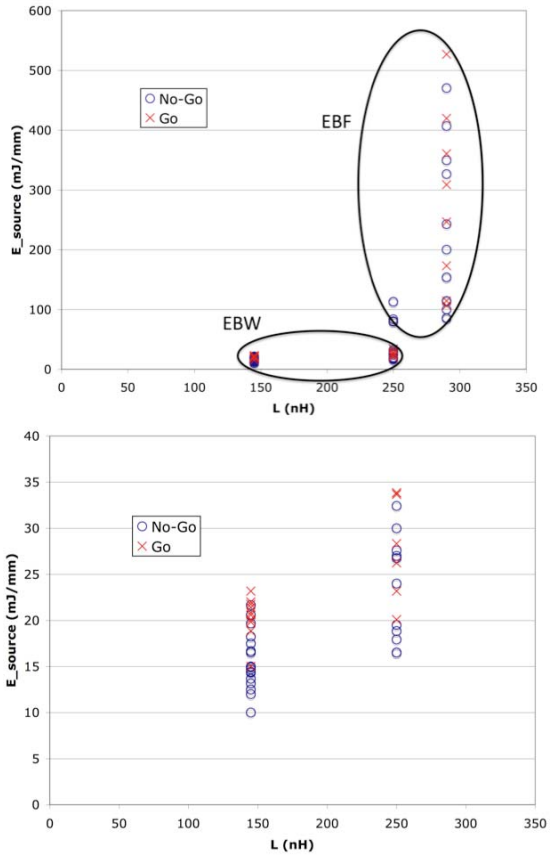

Fig. 2. Go/No-go test results from the historical LLNL experiments, normalized to energy per assumed shortest-path arc length, using firesets with three different inductances. The lower figure is a zoom-in of the EBW results from the upper.

The CVT waveforms were used to estimate the total circuit resistance (time-averaged) for a given shot. There was considerable shot-to-shot variation, with an average of about 40 Ω for the EBW configuration. Shorted ringdowns of the fireset showed an equivalent source resistance (ESR) of approximately 2 Ω, so most of the source energy was dissipated in the load. The measured current and the estimated resistance in turn allowed an estimate of the power delivered to the load.

Taking the test results at face value for the moment, it is not surprising that the power variation occurring as a result of varying inductance would influence the energy threshold. An HE sample bathed continuously by a light bulb (a limit of high total energy but very low power) is not going to react violently; neither, as experience bears out, will a sample that absorbs a single cosmic ray (a limit of high power but low total energy). Both energy and power must meet certain criteria for a reaction to take place. However, it is an open question as to what power levels are relevant to affect the behavior.

The "Tau Model"

As a starting point for the current work, we needed a simple model that would allow us to estimate the range of power variation that would be relevant for a new set of experiments. To that end, we consider an extremely simple physical description based on the following assumptions:

- On the time scale of the input pulse (tens of nanoseconds in a material not yet run to detonation), material motion can be ignored.
- For a violent reaction to ultimately occur, the local internal volumetric energy density E of the HE must exceed some critical value E_{crit}.
- Energy loss from any local volume is dominated by a single mechanism that is proportional to E and characterized by a time scale denoted by a constant, τ.[b]

With these assumptions, the full hydrodynamic equations reduce down to a single ODE for E as a function of time, given the temporal profile of the input power density, P:

$$\frac{dE}{dt} = P(t) - E/\tau \qquad (1)$$

For simplicity in both the loss term and the initial condition, we assume the relevant energy

[b] If this sounds too extreme, think of it as a local linearization of a more complicated energy transport mechanism. Note that even gradient-driven mechanisms tend to scale as ~ E/L where L is a scale length set by the geometry.

scale of E_{crit} is much greater than the ambient value of E at t=0. The general solution is then:

$$E(t) = \int_0^t P(t')e^{-(t-t')/\tau}dt' \qquad (2)$$

For several choices of P this is easily solved for an explicit threshold condition; for example, for a constant input pulse at power P_{in} over a time t_{in} corresponding to a total energy $E_{in} = P_{in}t_{in}$, one finds:

$$\frac{E}{E_{crit}} > \frac{P}{P_{crit}} \ln \frac{P/P_{crit}}{P/P_{crit} - 1} \qquad (3)$$

This condition has asymptotes at E_{crit} and $P_{crit}=E_{crit}/\tau$, as shown in Figure 3. The exact shape of the curve away from the asymptotes, as well as the definition of a single characteristic power, will in general vary depending on the temporal profile of the input power. The shape of the curve suggests an electrical analog to the highly successful James criterion for shock initiation,[6] although any two-asymptote model would likely bear a superficial resemblance.

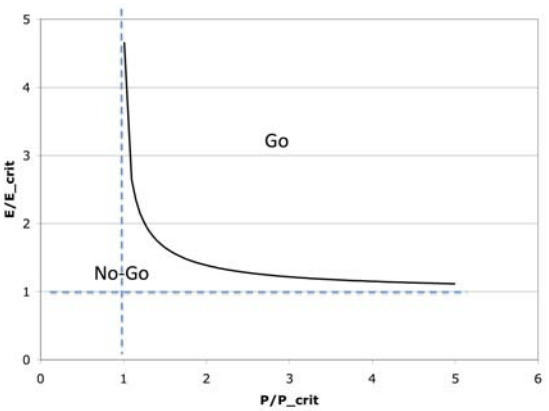

Fig. 3. Energy and power threshold curve from the "tau model" for the case of a square input power.

If we make the assumption that the transverse dimensions of point-to-point surface discharges in the regime of interest (millimeters of length, hundreds of millijoules of total energy, and megawatts of power) do not vary widely, then one would expect the observable power and energy thresholds to scale per unit arc length. Fitting the free parameters of the model, P_{crit} and E_{crit}, to the as-built EBW data (which has a simpler geometry that may justify a "shortest path" arc length) yields values of 0.5 MW/mm and 12 J/mm, respectively. The characteristic power for these waveforms is chosen to be the peak instantaneous power. These values guided the operational requirements of the fireset designed for our experiments, as described below.

Clearly, the assumptions made in the tau model are too strong to serve as a realistic model of ESD response of HE. A more fundamental approach, involving better characterization of both the properties of ESD-driven surface arcs and the resulting high-temperature kinetics of HE, can be found in the ongoing work of Grant and Tang.[7]

Fireset Hardware

The previous fireset designs in the historical tests focused heavily on achieving a particular goal for a single circuit parameter such as lower inductance. However, in doing so, other parameters critical to fireset performance were often traded away unintentionally.

The fireset developed for this work, as shown in Figure 4, was engineered to address two inherent shortcomings of the previous testing infrastructure: flexibility and control. The new fireset is able to cover a broad parameter space by allowing independently variable circuit capacitance and inductance at a maximum operating voltage of 30 kV. Thus, at 30 kV, the fireset can achieve stored energy levels from 30 mJ to 3.6 J and power levels from 1 MW to 80 MW.

The fireset can also accommodate a variety of high explosives in different forms. Powders can be pressed directly over the thin copper electrodes on the main stripline board, and pellets can placed over them at shot time. Small detonators can also have their leads attached to the flat stripline geometry with minimal additional inductance, if required.

Finally, the use of thin copper electrodes allows the fireset to have a well-defined arc path. Thus, this feature enables a degree of shot repeatability that is not possible when testing as-built components. (Visible-light images confirming the path definition and repeatability are

available.[7])

The main diagnostic on the fireset is a current-viewing resistor (CVR) integrated into the fireset circuit. Since the CVR is located close to the arc load, we assume that the current flowing through the CVR is the same as the load current.

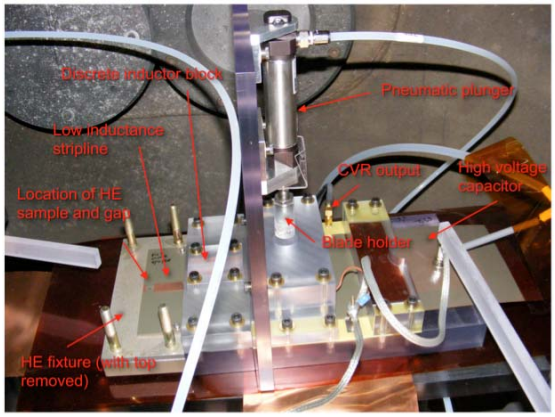

Fig. 4. The fireset developed for this work allows increased flexibility and control over the previous testing infrastructure.

Fireset Circuit Characterization

We developed a lumped-parameter predictive model of the fireset circuit to verify that its design satisfies experimental requirements and to help us design an efficient shot campaign. The model consists of five basic segments: the capacitor, the part of the stripline that feeds the capacitor into the switch, the part of the stripline from the switch to the inductor block, the inductor block itself, and the downstream portion of the stripline that feeds the arc load across the gap between the electrodes. The circuit model is shown in Figure 5.

The circuit model contains 22 parameters, and determining values for each of them appears, at first glance, to be a daunting task. However, due to the mostly flat geometry of the fireset, analytical expressions can be derived to predict the values of most circuit elements. In other words, most of the 22 parameters follow directly from fixed elements in the fireset geometry and do not change from shot to shot.

This leaves us with two main areas of uncertainty with regard to circuit parameters: the arc in the tack switch, and the arc load between the copper electrodes. For the former, we know that the arc length must be less than 30 mils, which is the spacing between the high- and low-side traces in the stripline. It is reasonable to assume that the inductance is bounded by the free-space value of 1 nH for this arc length; we use this value in all simulations. For the arc load, we assume a plausible range of inductance values from 1-5 nH for the 100-mil gap between electrodes, and we test several values within that range in our simulations to see their effect on the results.

In the absence of a reliable measurement of the voltage drop across the load, we assume that the switch resistance is a constant value represented by the observed fireset behavior when the load is shorted and the circuit ESR is minimized by using the smallest L and largest C available. We note that this effectively treats the switch resistance as independent of the operating parameters, which is unrealistic. Planned refinements to the stripline design will allow more easily allow characterization of the switch for each L and C combination used.

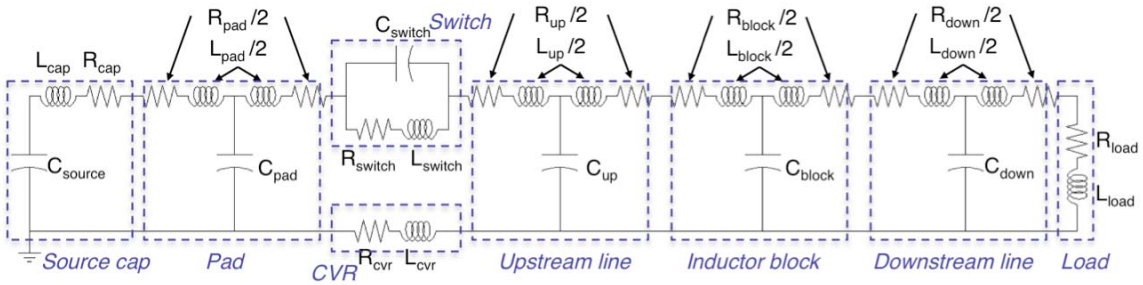

Fig. 5. Schematic of lumped-parameter model of the fireset circuit

The time-averaged arc load resistance is treated as an unknown parameter. As shown below, we find that using a constant resistance value in the modeling works surprisingly well to match the measured waveforms.

Model Output vs. Actual Data

Figures 6 and 7 show comparisons between the model output and actual shot data for two very different circuit inductances. In both cases, the model and data agree well, and the model is able to capture the high-frequency content contributed by the switch and load inductances.

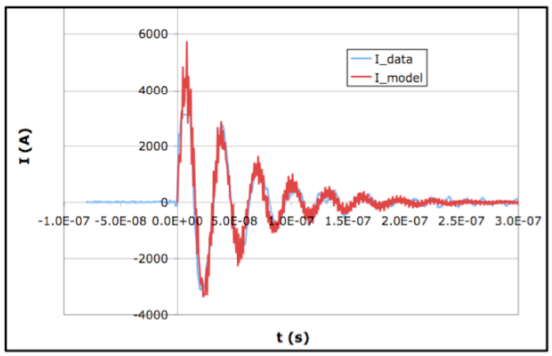

Fig. 6. Comparison between model output and actual data for a 30 nH shot.

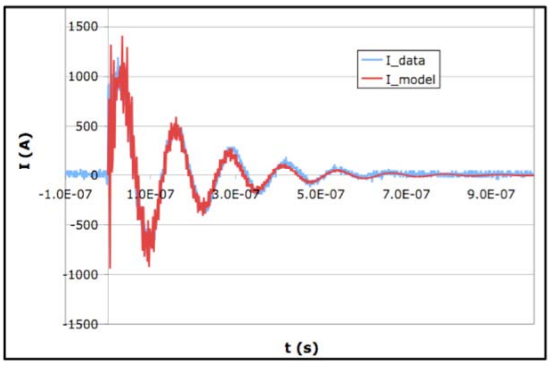

Fig. 7. Comparison between model output and actual data for a 540 nH shot.

Experiments and Results

Our experiments were designed to explore variations in energy threshold when different parameters were varied including arc length, powder surface area, surface vs. bulk discharge paths, and power delivered to the arc load. We treat each of these parameters individually in this section.

Baseline Test Series

We did a series of threshold tests using 100-mil (about 2.5 mm) surface arcs in 50% TMD PETN with BET surface area of 0.83 m^2/g and used the data as our baseline data set. The results are shown in Figure 8 and are presented as a function of source energy with peak power on the vertical axis. We calculate peak power by matching the data to a fitted RLC circuit model and obtaining a fitted value for the load resistance.

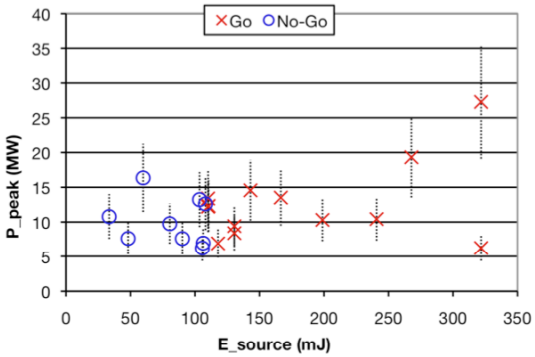

Fig. 8. Baseline data set using 100-mil surface arcs in 50% TMD PETN with BET surface area of 0.83 m^2/g. The mean is 109.7 mJ with a standard deviation of less than 1.0 mJ.

Fig. 9. Typical appearance of a no-go, showing compression (and not reaction, as determined by weight).

The mean energy threshold is 109.7 mJ

with a standard deviation of less than 1.0 mJ due to the lack of crossover in the data. Multiple shots on either side of the tight threshold found it remarkably robust. Data from subsequent test series that look at the various parameters mentioned earlier are compared against these results.

The typical appearance of a no-go is shown in Figure 9. One can see clear evidence of compression (not reaction, as verified by comparing pre- and post-shot sample weights) but no indication of violence. In contrast, Figure 10 shows a typical post-shot result. Since we do not distinguish between violent response and full detonation in our safety studies, the differences between a go and a no-go are unambiguous in PETN.

Fig. 10. Typical appearance of a go, showing destruction of the collar confining the powder and some cracking of the Lexan holder.

Length Scaling

A fundamental assumption in mapping threshold data from one arc geometry to another is that the energy threshold will scale per unit length of arc path since the underlying physical response of the HE is dependent on an energy density. We add to this the caveat that the variation in arc length and timescale cannot be too different for what we consider a "typical" short-length, high-power ESD discharge; otherwise, the more three-dimensional character of the arc will become important.

To explore variations in energy threshold with varying arc length, we did a test series using 50-mil surface arcs in 50% TMD PETN with BET surface area of 0.88 m^2/g. The results of this test series are shown in Figure 11. The mean energy threshold is 48.2 mJ with a standard deviation of 6.8 mJ.

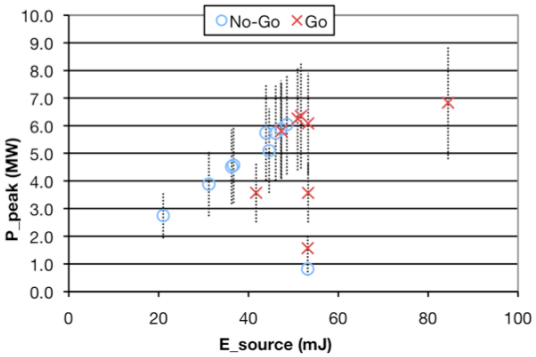

Fig. 11. 50-mil surface arcs in 50% TMD PETN with BET surface area of 0.88 m^2/g. The mean is 48.2 mJ with a standard deviation of 6.8 mJ.

The major conclusion from this test series is that arc length is indeed a strong parameter, and the energy threshold scales in proportion. In other words, the threshold can be properly defined in terms of the energy per unit arc length.

We also make a general observation about the diagonal trend of the data below 45 mJ in Figure 11. The fireset can tune energy and power independently because it has the ability to decrease circuit inductance as the energy is lowered to keep the power high. However, in this shot series we reached the lowest-inductance configuration of the fireset at about 45 mJ and no longer had the means to maintain high power levels. Thus at 45 mJ, both energy and power begin to scale linearly with capacitance and with the square of the voltage.

Scaling With Powder Surface Area

A second test series using 100-mil surface arcs in 50% TMD PETN was performed, but in this series the BET surface area of the powder was 0.70 m^2/g. The results are shown in Figure 12. For shots above 8 MW, the mean energy threshold is 118 mJ with a standard deviation of 13 mJ. The shots below 8 MW are discussed in the section *Power Delivered to Arc Load* below.

We note that the overlap in this series is considerable, in sharp contrast to the baseline case; there is some indication that the inductor blocks were becoming susceptible to breakdown with repeated use, leading to parasitic energy loss.

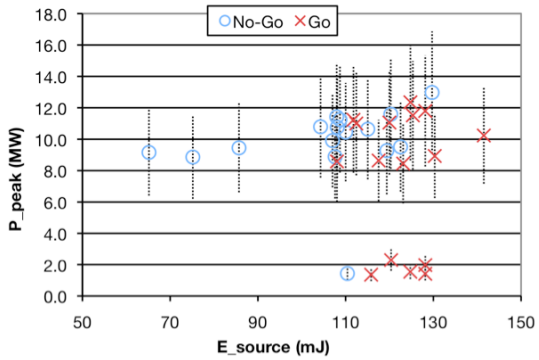

Fig. 12. 100-mil surface arcs in 50% TMD PETN with BET surface area of 0.70 m^2/g. The mean for shots above 8 MW is 118 mJ with a standard deviation of 13 mJ.

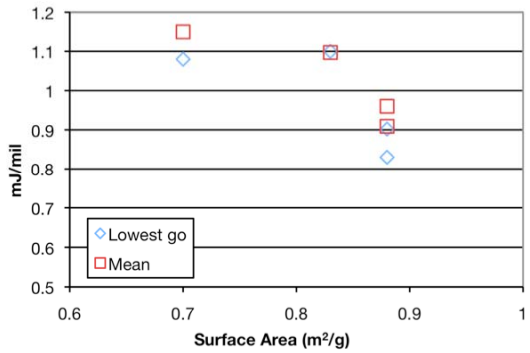

Fig. 13. Normalized energy thresholds as a function of powder specific surface area (measured via BET).

Although the available data set is rather small, it does support a dependence on the BET surface area of the powder. Figure 13 plots the mean energy thresholds for all test series against the specific surface area of the powder used. The slope appears similar to that indicated in the results of Tucker,[5] although a quantitative comparison is difficult since the powder characterization method for those tests is not explicitly stated and is likely to have been Fischer rather than BET. For the PETN powders used in our tests, the mean energy threshold is in the neighborhood of 1 mJ per mil of arc length.

Surface vs. Bulk Discharge Paths

In the as-built component testing, the presumption was that the pin-to-cap breakdown occurs along the surface, although this has not been proven. To address the question of whether a bulk breakdown of PETN can produce behavior different from a surface arc, we did a test series using electrodes that were separated by a 100-mil gap and buried through a two-step pressing process in 50% TMD PETN with BET surface area of 0.88 m^2/g. The results of this test series are shown in Figure 14. The mean energy threshold is 120 mJ with a standard deviation of 10 mJ.

The mean threshold is not significantly different from the baseline test case. Due to the mechanics of realizing the buried-electrode configuration, there was a marked increased in the overall circuit resistance and inductance, which likely caused the mean threshold to be higher than what one might conclude from the section *Scaling With Powder Surface Area* above.

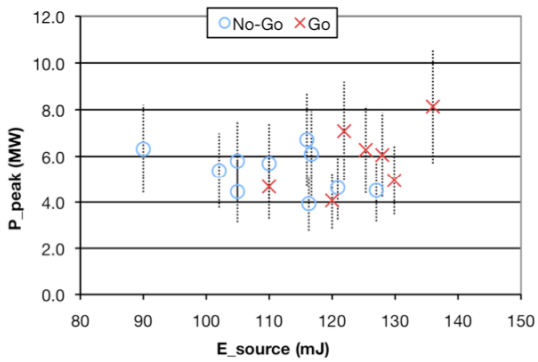

Fig. 14. 100-mil arcs buried in 50% TMD PETN with BET surface area of 0.88 m^2/g. The mean is 120 mJ with a standard deviation of 10 mJ.

Power Delivered to Arc Load

Because our fireset has the ability to tune energy and power independently, we made

several attempts to find an explicit threshold in power rather than energy, as the tau model would indicate.

In the 50-mil surface arc test series shown in Figure 11, we did a sequence of shots at constant source energy of about 53 mJ. The results are tantalizing but misleading for reasons presented shortly.

Another "vertical walk" in power was attempted in the test series using 0.70 m^2/g powder as shown in Figure 12. Since the mean energy threshold for this test series is 118 mJ, we chose the constant energy level to be 128 mJ, which is just under one standard deviation above the mean. However, two shots fired using the largest available inductor of 1.5 µH—and thus the lowest power the fireset could produce at fixed energy—were both goes. The decision was made to walk downwards in energy at low power, and as seen in Figure 12, all but one such shot was a go with the transition consistent with the mean found at high power. In fact, if the energy threshold calculation included both low- and high-power shots, the resulting mean is only slightly different from the value reported above: 114 mJ with a standard deviation of 7.6 mJ.

The lack of observed power dependence over a variation of almost an order of magnitude in power weakens the foundation for the tau model, at least in the regime consistent with the posited inductance dependence of the as-built test data. The power threshold must be at a level significantly lower than what is relevant to either these or the as-built experiments.

This conclusion is corroborated by the consistency with which the low-power shots in both test series agree with the high-power energy threshold. In the 50-mil surface arc shots, it is tantalizing to treat the one no-go in the constant energy series at 53 mJ as evidence of a possible power threshold at around 1.5 MW. However, since power scales per unit length (because the arc resistance scales per unit length), a 1.5 MW power threshold for a 50-mil arc would imply a 3 MW power threshold for a 100-mil arc. However, the evidence does not support this conclusion because all of our low-power 100-mil surface arcs were done below 3 MW. It is most likely the no-go is simply a reflection of energy threshold distribution as affected by the inductor block losses mentioned earlier.

PBX 9407 Experiments

The "shortest path" argument of pin-to-cap surface arcs, as applied to the as-built EBF detonator tests, would indicate that the HE that first reacted in those tests was PBX 9407 and not PETN. We conducted a number of experiments on PBX 9407 pellets to obtain results where the reacting HE was unambiguous.

Using large commercial 8.3-nF high-voltage capacitors, four types of experiments were performed: 1) 100-mil surface arcs at various power levels; 2) a less robust version of the bulk breakdown tests for PETN in that the electrodes were simply held in place between two pellets; 3) a somewhat more robust version of the previous test in which very small holes (measuring approximately 90 x 40 µm) were drilled axially to serve as a starter path for an arc through the pellet; and 4) a cook-off experiment using the maximum 750 µA output of the high-voltage supply to sustain a 100-mil arc under a pellet for five minutes. A summary of results from these tests is shown in Figure 15; note the high insult energy compared to the PETN shots.

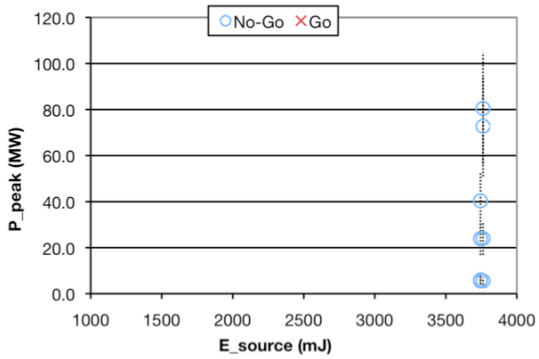

Fig. 15. Summary of results from various shot configurations using PBX 9407.

All shots and the cook-off were no-goes, which indicates that PBX 9407 was not the

reacting material in the as-built EBF detonator tests (at least for the source energies employed in those tests). Post-shot inspection of the pellets revealed some cracking and discoloration, but no sign of any violent reaction. Figure 16 shows a picture of a pellet after it received an arc insult.

Fig. 16. Picture of a PBX 9407 pellet after receiving a high-energy, high-power arc insult.

Summary

Some historical test results of high-power ESD pin-to-cap insults to EBW and EBF detonators indicated the possibility of a significant power dependence to the response threshold of low-density PETN. There was also evidence that in this high-power regime it was possible to initiate high-density secondary explosives (in this case, PBX 9407) with relatively low insult energies. To explore this behavior, we have performed an extensive series of tests using a fireset designed to furnish insults easily cast in terms of electrical energy and power, rather than specific circuit parameters, and to do so with a well-defined arc path either across or through the HE under test. We have observed in low-density PETN a linear scaling of energy threshold with arc length, no strong dependence on bulk versus surface discharges, and decreasing threshold with increasing specific surface area. In the same range of powers as the historical tests, we have not observed any significant dependence on power and postulate that the variation seen in the historical tests is due to variation in breakdown path and energy delivered to the load (even at fixed source energy). In tests involving only PBX 9407, we were unable to initiate a violent reaction even at insult energies considerably higher than used in the historical tests; we take this as evidence that the breakdown path in the EBF configuration of those tests was not the shortest geometrical path but one that must have crossed PETN.

Acknowledgments

This work performed under the auspices of the U.S. Department of Energy by Lawrence Livermore National Laboratory under Contract DE-AC52-07NA27344.

References

1. Asay, B.W. (ed.), *Shock Wave Science and Technology Reference Library Vol. 5: Non-Shock Initiation of Explosives*, Springer-Verlag, Berlin, 2010.
2. Steich, D., private communication, Lawrence Livermore National Laboratory, Livermore, CA 94551.
3. Fisher, R.J, "A severe human ESD model for safety and high reliability system qualification testing," in *Proceedings of the 1989 EOS/ESD Symposium*, New Orleans, 1989.
4. IEEE Std. C62-47 1992, "IEEE Guide on Electrostatic Discharge (ESD): Characterization of the ESD Environment," Institute of Electrical and Electronics Engineers, New York.
5. Tucker, T., Kennedy, J., Allensworth, D., "Secondary Explosive Spark Detonators," in *Proceedings of the 7th Symposium on Explosives and Pyrotechnics*, The Franklin Institute Research Laboratories, Philadelphia, PA, Sept 8-9, 1971.
6. James, H. R., "An Extension to the Critical Energy Criterion Used to Predict Shock Initiation Thresholds," in *Propellants, Explosives, Pyrotechnics 21*, 1996, pp. 8-13.
7. Grant, C., Tang, V., McCarrick, J., Glascoe, E., "Towards the understanding of initiation of PETN by a fast, high-power arc source," these proceedings.